*Journal of the Korean Electrochemical Society*
*Vol. 9, No. 4, 2006, 158-169*

# An Overview of Chemically/Surface Modified Cubic Spinel $LiMn_2O_4$ Electrode for Rechargeable Lithium Batteries

Kyu-Nam Jung and Su-Il Pyun*

*Department of Materials Science and Engineering, Korea Advanced Institute of Science and Technology, 373-1 Guseong-Dong, Yuseong-Gu, Daejeon 305-701, Korea*

(Received October 17, 2006 : Accepted October 24, 2006)

**Abstract** : The present article is concerned with the overview of the chemically/surface modified cubic spinel $LiMn_2O_4$ as a cathode electrode for lithium ion secondary batteries. Firstly, this article presented a comprehensive survey of the cubic spinel structure and its correlated electrochemical behaviour of $LiMn_2O_4$. Subsequently, the various kinds of the chemically/surface modified $LiMn_2O_4$ and their electrochemical characteristics were discussed in detail. Finally, this article reviewed our recent research works published on the mechanism of lithium transport through the chemically/surface modified $Li_{1-\delta}Mn_2O_4$ electrode from the kinetic view point by the analyses of the experimental potentiostatic current transients and ac-impedance spectra.

**Key words :** $LiMn_2O_4$ Electrode, Cubic Spinel Structure, Chemically/Surface Modified Electrode, Cell-impedance-controlled Lithium Transport, Lithium Batteries.

## 1. Introduction

Cubic spinel $LiMn_2O_4$ has been considered to be the most promising alternative cathode material for new generation of lithium ion batteries because of its low cost, low toxicity and easy manufacturing.[1,2] Unfortunately, $LiMn_2O_4$ electrode in the high potential region severely suffers from the capacity fading, especially at elevated temperature, due mainly to the detrimental surface reactions with acidic contaminants in the electrolyte solutions and to the detrimental structural changes of the active material caused by the dissolution of manganese.[3,4]

To circumvent these problems, earlier studies have been focussed on the structural stability of $LiMn_2O_4$ such as cationic substitutions for manganese and on reduction of specific surface area of the active material to reduce active surface area exposed to the electrolyte and its contaminants.[5-9] However, these approaches reach uppermost limit and the capacity fading can not be overcome fully at elevated temperature. In order to further improve the capacity fading of $LiMn_2O_4$, a great interest has been focussed on the surface-modification of $LiMn_2O_4$ with oxide materials such as $Al_2O_3$, $LiCoO_2$, MgO, ZnO and $ZrO_2$,[10-17] because the interface between the electrolyte and active material plays a significant role in the battery processes.

The objective of this article is to overview the chemically/surface modified cubic spinel $LiMn_2O_4$ electrode as a cathode material for rechargeable lithium batteries. For this purpose, we firstly introduced a comprehensive survey of the cubic spinel structure and its correlated electrochemical properties of $LiMn_2O_4$. Secondly, we presented the various kinds of the chemically/surface modified $LiMn_2O_4$ and then gave the detailed discussion about their electrochemical behaviour. Finally, based upon our recent works, this article reviewed the mechanism transition of lithium transport through the chemically/surface modified $Li_{1-\delta}Mn_2O_4$ electrode by analyses of the potentiostatic current transients and ac-impedance spectra experimentally measured.

*E-mail: sipyun@webmail.kaist.ac.kr

## 2. Cubic Spinel Structure and its Correlations with Electrochemical Properties of $LiMn_2O_4$

### 2.1 Cubic Spinel Structure of $LiMn_2O_4$

Over the last two decades, many transition metal oxides such as titanium, vanadium, manganese, iron, cobalt and nickel oxides have been investigated as insertion electrodes for lithium batteries. From the practical view point that lithium manganese oxides can offer a wide selection of materials, much attentions have been paid to lithium manganese oxide systems with various types of structure.[2,18] Moreover, since lithium manganese oxides are inexpensive and non-toxic as compared to the other transition metal oxides and provide voltages up to 5 $V_{Li/Li+}$, they have been considered as candidate cathode materials for lithium batteries. Especially, cubic spinel $LiMn_2O_4$ with space group symmetry Fd3m is of particular interest because $Mn_2O_4$ spinel framework provides an uninterrupted and energetically accessible three-dimensional interstitial space of face-sharing tetrahedra and octahedra for lithium ion diffusion through the structure.[2]

The ideal spinel ($LiMn_2O_4$) structure consists of an fcc

oxygen packing in which lithium ions, manganese ions and oxygen ions locate on the 8a tetrahedral sites, 16d octahedral sites and 32e positions of Fd3m space group, respectively as shown in Fig. 1(a). When lithium ions are intercalated into $Mn_2O_4$ framework, they only reside in the 8a tetrahedral sites. It should be noted that in the spinel structure $MnO_6$ octahedra are edge-shared and form a continuous three-dimensional cubic-array, thereby providing a stability of $Mn_2O_4$ spinel framework. In addition, the 8a tetrahedra sharing each of four faces with adjacent 16c octahedra are situated farthest from the 16d octahedra occupied by manganese in all the interstitial tetrahedra (8a, 8b and 48f) and octahedra (16c).

The 8a and 16c sites form a three-dimensional pathway for lithium ion diffusion. When lithium ions are further intercalated into $LiMn_2O_4$ composition, only the octahedral 16c sites are available. Since the electrostatic repulsion between the intercalated lithium ions is so high that a migration of lithium ion from the 8a sites to the 16c sites occurs, which leads to $(Li_2)_{16c}(Mn_2)_{16d}(O_4)_{32e}$ rock salt type composition. Fig. 1(b) and (c) shows the structure of cubic spinel $LiMn_2O_4$ framework representing the octahedral and tetrahedral coordination of lithium ions and three-dimensional interstitial pathway for lithium ion diffusion, respectively.

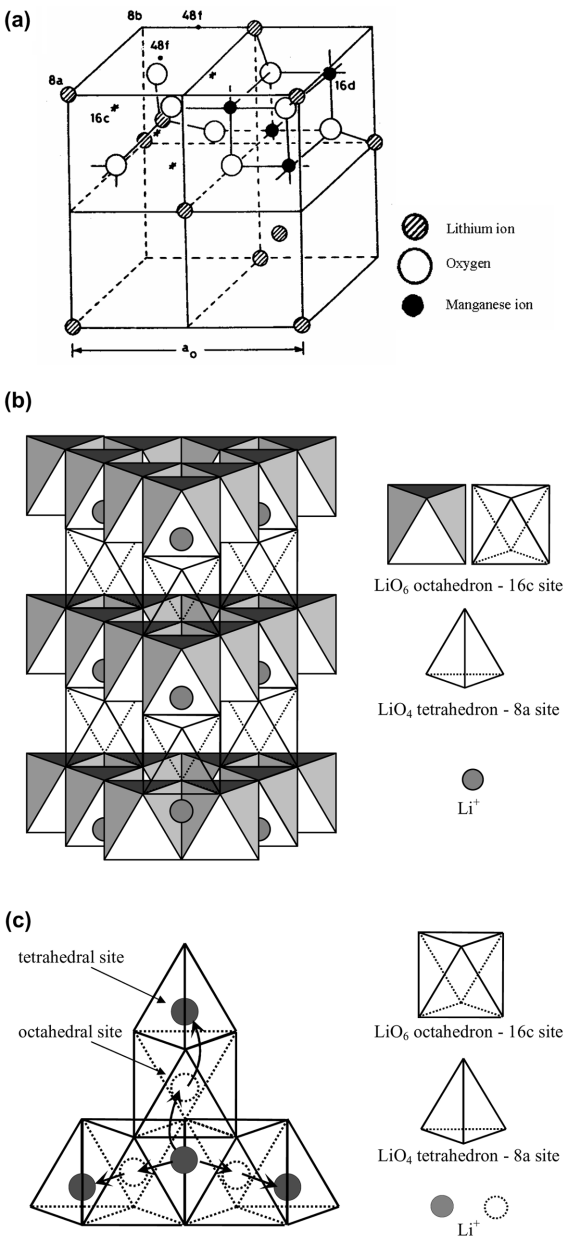


**Fig. 1. Schematic diagrams (a) for the cubic spinel $LiMn_2O_4$ structure with space group Fd3m, (b) for stacking of $LiO_6$ octahedra and $LiO_4$ tetrahedra and (c) for diffusion path of lithium ion through the chain of $LiO_6$ octahedra and $LiO_4$ tetrahedra.**

### 2.2 Correlations of Cubic Spinel Structure with Electrochemical Properties of $LiMn_2O_4$

The electrochemical behaviour of $LiMn_2O_4$ electrode is strongly related to the structural properties of the material. It was reported[2] that the electrode potential depends not only on the formal valence-state of manganese ions, but also on the relative energy of lithium sites in the various structures, implying that high potentials of $LiMn_2O_4$ are associated with increasing difficulty in removing lithium ion from a particular site with the deepest energy well during the lithium intercalation and deintercalation.

The reversible lithium intercalation and deintercalation into and from $Li_xMn_2O_4$ spinel phase occur and hence give rise to two voltage plateaus located at ca. 4 and 3 $V_{Li/Li+}$ in two compositional ranges, $0 \le x \le 1$ and $1 \le x \le 2$, respectively. Over the compositional range $0 \le (1-\delta) \le 1$ in $Li_{1-\delta}Mn_2O_4$, it was reported that lithium is deintercalated from the tetrahedral sites of the spinel structure at approximately 4 $V_{Li/Li+}$ in a two-stage process, separated by only 150 mV at the lithium content of $Li_{0.5}Mn_2O_4$.[19] This two-stage process reaction is known to be due to the ordering of lithium ions on one half of the tetrahedral 8a sites.[20-22] The high voltage associated with these two reactions can be attributed to the deep energy well in which the tetrahedral lithium ions reside, and the high activation energy that is required for lithium ion to move from one 8a tetrahedron into another 8a site via an energetically unfavourable neighbouring 16c octahedron as shown in Fig. 2(a).[2]

Further lithium intercalation occurs into $Li_{1+\delta}Mn_2O_4$ (over

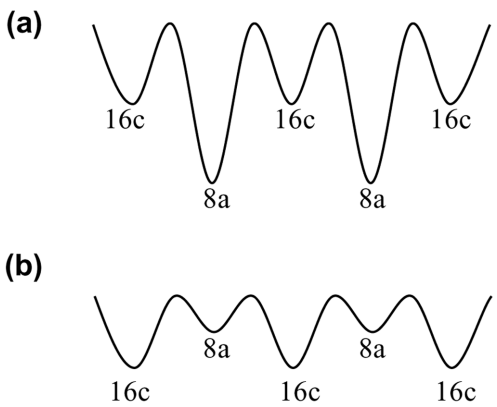


**Fig. 2. Schematic representation of the difference in site energies for the 8a tetrahedral sites and 16c octahedral sites (a) in cubic spinel $LiMn_2O_4$, and (b) in rock salt phase $Li_2Mn_2O_4$.**

the compositional range $1 \leq (1+\delta) \leq 2$) at approximately 3 $V_{Li/Li+}$. During this process, lithium ions are intercalated into the octahedral 16c sites of the spinel structure. Because the 16c octahedra share faces with the 8a tetrahedra, the electronic interactions between lithium ions on these two sets of sites cause an immediate displacement of lithium ions at the tetrahedral site into neighbouring vacant 16c octahedral.[2] The reaction results in a first-order transition to $Li_2Mn_2O_4$ with a stoichiometric rock salt composition on the surface of the electrode. Thus, the electrode potential curve of $Li_{1+\delta}Mn_2O_4$ at the potential of 3 $V_{Li/Li+}$ shows the potential plateau.

During the lithium intercalation, a reaction front of $Li_2Mn_2O_4$ may form and move progressively from the surface of the electrode into the bulk. In the rock salt structure, the octahedral 16c sites are of lower energy than the tetrahedral 8a sites as depicted schematically in Fig. 2(b). It was known that lithium ions may be distributed on both the 8a and 16c sites of the spinel structure at rock salt composition. This implies that the difference in site energy between the octahedral and tetrahedral sites is relatively small and thus less energy is required to remove lithium ion from the octahedral sites of $Li_2Mn_2O_4$ rock salt phase than from the tetrahedral sites of $LiMn_2O_4$ spinel phase. This result suggests that a lower activation energy for lithium ion diffusion can be expected for the rock salt phase as compared to the spinel phase.[2,23]

In the case of the lithium intercalation into $Li_{1+\delta}Mn_2O_4$ electrode at 3 $V_{Li/Li+}$, a severe Jahn-Teller distortion occurs as a result of an increased concentration of $Mn^{3+}$ ions in $Mn_2O_4$ spinel framework. It reduces the crystal symmetry from cubic (c/a=1.0) to tetragonal symmetry (c/a=1.16).[24] The increase of c/a ratio is too severe for the spinel structure to withstand lithium transport through the structure during the cycling. The strain imposed on the system is too great for the individual spinel particles to maintain structural integrity. Accordingly, they tend to break up and lose electrical contact, thereby resulting in rapid capacity loss of the electrode.[2]

Although cubic spinel $Li_{1-\delta}Mn_2O_4$ in the potential range of 4 $V_{Li/Li+}$ is significantly more tolerant to the cycling than that in the potential range of 3 $V_{Li/Li+}$, slow capacity fading is encountered in the potential range of 4 $V_{Li/Li+}$. There are several main factors responsible for this capacity fading[2]:

(i) dissolution of manganese from the spinel electrode in the acidic electrolyte. $Mn^{3+}$ dissolution occurs by a disproportionation reaction as follows:

$$2Mn^{3+}(solid) \rightarrow Mn^{4+}(solid) + Mn^{2+}(solution) \quad (1)$$

(ii) electrolyte decomposition. Since $Mn^{4+}$ ions have a high oxidation ability, the non-aqueous electrolyte can easily decompose at the high potential region. This reaction can lead to manganese dissolution.

(iii) Jahn-Teller distortion at the end of discharge. Under dynamic conditions, the surface of the electrode particles can easily reach an overdischarged composition, in which the average oxidation state falls below 3.5.

There have been several efforts to overcome those problems of $LiMn_2O_4$ by modifying the composition of the spinel. In order to stabilise the spinel structure of $LiMn_2O_4$, a small fraction of manganese ions in $LiMn_2O_4$ framework is replaced by lithium.[5] These lithium-substituted spinel electrodes can be represented by general formula $Li_{1+x}Mn_{2-x}O_4$. Fig. 3 shows the plots of the lithium content ($1+x$), manganese oxidation state and capacity loss against the lattice parameter of cubic spinel $Li_{1+x}Mn_{2-x}O_4$.[25] As the lattice parameter decreases, the lithium content and manganese oxidation state increase, and the capacity loss decreases. This means that the lithium-substituted spinel electrodes exhibit improved cycling properties because the increased concentration of $Mn^{4+}$ in the electrode inhibits the dissolution of $Mn^{3+}$ and simultaneously onset of the Jahn-Teller effect.

In a manner similar to the lithium-substituted spinel electrode, divalent or trivalent cations such as $Co^{2+}$, $Mg^{2+}$, $Ni^{2+}$, $Zn^{2+}$ and $Cr^{3+}$ [5-9] are substituted for manganese to increase the mean oxidation state of manganese ion. For example, $LiMn_{1.975}Mg_{0.025}O_4$ with an average manganese oxidation

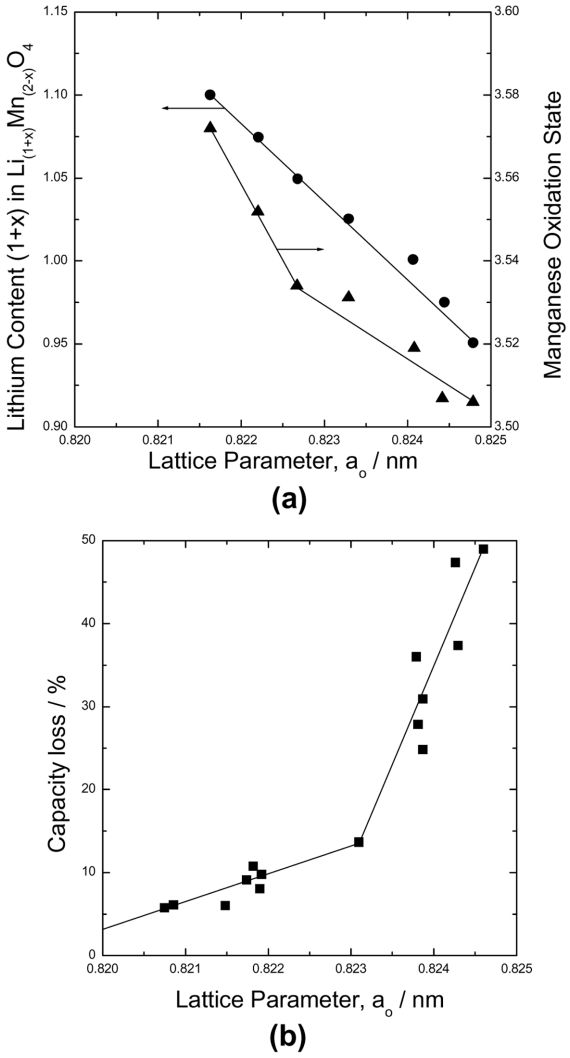


**Fig. 3. Plots of (a) the lithium content ($1+x$) and manganese oxidation state and (b) the capacity loss against the lattice parameter of cubic spinel $Li_{1+x}Mn_{2-x}O_4$.[25]**

state of 3.52 shows the enhanced capacity retention similar to that obtained from $LiMn_{1.97}Li_{0.03}O_4$.[5] However, these cation-substituted spinel electrodes show the reduced initial cell capacity, since the initial capacity of the cells is determined by the average manganese oxidation state.

These cationic substitutions for manganese are now at the end of their rope and the problem of the capacity fading can not completely be solved. Thus, in order to further improve the capacity fading of $LiMn_2O_4$, a great interest has been recently paid to the chemically/surface modified $LiMn_2O_4$ with metal oxides.

## 3. Chemically/Surface Modified Cubic Spinel $LiMn_2O_4$

### 3.1 Chemically Modified Electrode

The concept of 'chemically modified electrode'(CME) was born in the mid 70's when Murray and co-workers achieved the functionalisation of $SnO_2$ electrode surface with amine groups.[26] This pioneering work is the starting point for the development of an extraordinary wide area of research which is still continuously growing in various fields of electrochemistry.[27-29] The origin of this success should be found in the numerous possibilities of intelligently designing the surface of the conventional electrodes to improve their response by combining the intrinsic properties of the modifier to a selected electrochemical reaction.

CME can be divided into four main categories base upon the nature of modifying process by Murray's assignment: sorption-based CME, covalently modified electrode, homogeneous multilayer CME and heterogeneous multilayer CME. In the case of the sorption-based CME, the physical and chemical interaction properties are utilised to form monolayer structures during the modification procedures. The chemisorbed thiols self-assembled monolayer on Au surface is well-known example in sorption studies.[30] Covalent modification of the electrode surface by using specific functional group is also of particular interest in the preparation of CME. For example, >C=O and >C-O$^-$ functional groups formed on glassy carbon electrode and –OH groups from oxide electrode are often utilised in various applications.[31,32] In addition, the homogeneous multilayer CME can be prepared by using redox polymers and inorganic polymers.[28]

In the case of the heterogeneous multilayer CME, the various inorganic materials including metal oxides,[33,34] clay,[35] zeolite[36] and silica gel[37] have been considered as the modifying agent of the conventional electrode. Some of unique characteristics such as ion exchange property and intrinsic catalytic activity of clay and zeolite can be applied to the amperometric sensors[38] and biosensors[39] in the analytical chemistry.

### 3.2 Various Kinds of Chemically/Surface Modified $LiMn_2O_4$ Electrode and its Electrochemical Behaviour

Based upon the fact that Mn dissolution occurs at the interface between the electrolyte and $LiMn_2O_4$ electrode, Tarascon *et al*. proposed[40] that the easiest way to improve the electrochemical performance is to fabricate a material with low surface area. However, large particles with low surface area may reduce the rate of lithium diffusion through the spinel, which results in the limitation of high rate capability of $LiMn_2O_4$, and may causes the separator penetration and subsequent formation of short circuits.

Thus, in order to decrease the surface area exposed to the electrolyte, inorganic $Li_2O{\cdot}2B_2O_3$ (LBO) glass is coated on $LiMn_2O_4$.[8] Coated LBO glass protects the electrolyte from the catalytic effects and prevents $LiMn_2O_4$ from the corrosion of HF. In addition, since LBO has the good wetting property, high ionic conductivity, thermal stability and structural stability against high oxidation potentials in the potential range of 4 $V_{Li/Li+}$, the LBO-modified $LiMn_2O_4$ exhibits the improved storage properties at high temperature. However, the LBO-modified $LiMn_2O_4$ shows the poor cycling properties at elevated temperatures, since $LiMn_2O_4$ is likely to form solid solutions with borate compounds.[8]

$Al_2O_3$ is coated on $LiMn_2O_4$ by sol-gel procedure.[11] The capacity retention of the $Al_2O_3$-modified $LiMn_2O_4$ is more than 85% after 100 cycles at high temperature as shown in Fig. 4(a). It was suggested that $Al^{3+}$ ions replace $Mn^{3+}$ ions in the spinel lattice and the solid solution film of $LiMn_{2-x}Al_xO_4$ is formed on the electrode surface. This solid solution film improves the structural stability of $LiMn_2O_4$ by reducing the structural degradation of $LiMn_2O_4$ at elevated temperature.

$LiCoO_2$ can also be deposited on $LiMn_2O_4$ surface by using sol-gel method, micro-emulsion method and electrostatic spray deposition technique.[10-12] It was reported that the structural stability during the cycling at high temperature is markedly improved due to the suppression of Mn dissolution, since high concentration Co ions at the surface play a significant role in protecting the active material from $Mn^{3+}$ dissolution in the electrolyte. Moreover, the cycling performance of the $LiCoO_2$-modified $LiMn_2O_4$ at high temperature is greatly improved.

For example, the $LiCoO_2$-modified $LiMn_2O_4$ shows higher capacity retention than that of the unmodified $LiMn_2O_4$ as shown in Fig. 4(a).[11] The former electrode maintains ca. 92% of maximum capacity at 0.5 C rate after 100 cycles, whereas the latter electrode just maintains ca. 58% of maximum capacity. However, the rate capability of the $LiCoO_2$-modified $LiMn_2O_4$ is slightly reduced due to the increase of lithium diffusion resistance caused by the protective $LiCoO_2$ film. Furthermore, Kannan and Manthiram proposed[11] that the $LiCoO_2$-modified $LiMn_2O_4$ heated at high temperature of 850°C can be considered as the chemically modified electrode since the guest ions will diffuse into the bulk of the host lattice at high processing temperature to give phases such as $LiMn_{2-2x}Li_xCo_xO_4$.

MgO-modified $LiMn_2O_4$ is prepared by the sonochemical method.[13] The sonication of slurries being composed of $LiMn_2O_4$ particles and magnesium sources such as $MgSO_4$ or Mg acetate, produces $LiMn_2O_4$ coated by $Mg(OH)_2$ film and then heat treatment at 450°C transforms $Mg(OH)_2$ to MgO. Especially, the capacity retention of the MgO-modified $LiMn_2O_4$ is greatly improved as compared to the unmodified

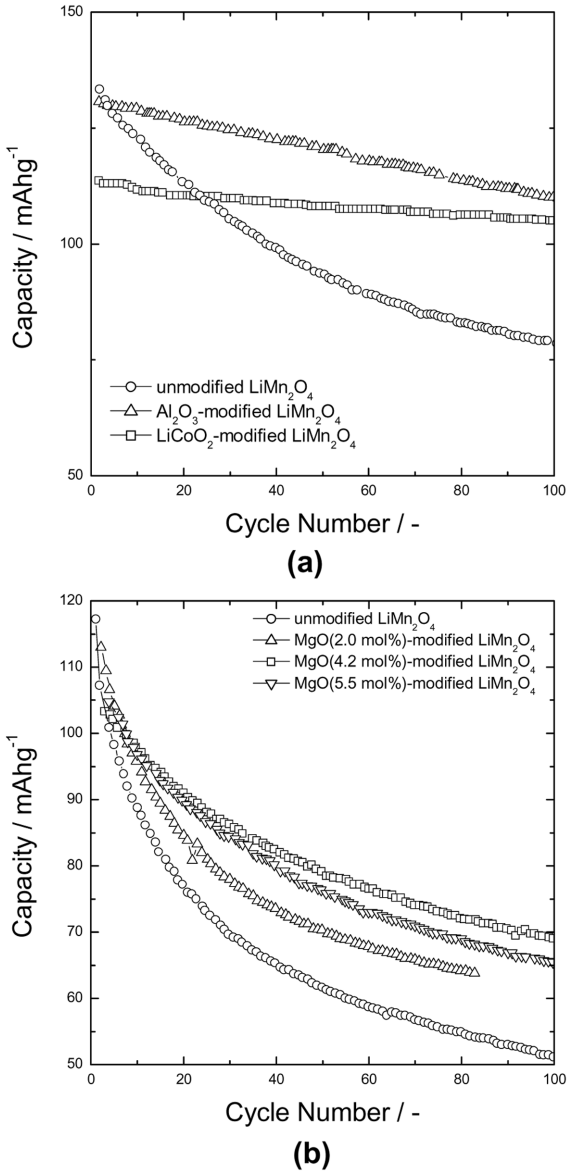


**Fig. 4. Plots of the capacity against the cycle number obtained (a) from the unmodified and chemically modified $LiMn_2O_4$ with $Al_2O_3$ and $LiCoO_2$ electrodes in a 1 M $LiPF_6$-EC/DEC,[11] and (b) from the unmodified and chemically modified $LiMn_2O_4$ electrodes with various amounts of MgO in a 1 M $LiPF_6$-EC/DEC/DMC at 60°C.[13]**

$LiMn_2O_4$ at high temperature as shown in Fig. 4(b). Aurbach *et al*. proposed[13] that MgO film, which is so porous that lithium ions can freely diffuse into the active material, protects $LiMn_2O_4$ from the detrimental reactions with acidic solution species (HF in the electrolyte). These solution species usually form resistive surface films that increase the resistance of the electrode.

Moreover, the improvement in the capacity fading and cycling stability can also be achieved by coating colloidal nano-particles of $ZrO_2$ on the spinel $LiMn_2O_4$ surface. Thackeray *et al*. reported[41] that $ZrO_2$ particles neutralise HF-component in the non-aqueous electrolyte and hence the $ZrO_2$-modified $LiMn_2O_4$ shows the enhanced electrochemical performance at 50°C. In addition, the increase of the discharge capacity has been ascribed to strong Zr-O bonds at the electrode surface that contribute to decrease of the oxygen activity of the electrode surface at high potentials.

It is clear that the coated inorganic oxides can modify the properties of the surface exposed to the electrolyte and can enhance the electrochemical properties and structural stability of $LiMn_2O_4$. However, the available capacity of the surface modified materials is lower than that of the active material because of the formation of electrochemically inactive compounds in the coating layer. Thus, there are new challenges to coat the organic polymer such as poly(diallyldimethyl-ammonium chloride) (PDDA), poly(3,4-ethylenedioxy)thiophene (PEDOT) and polypyrrole (PPy) on $LiMn_2O_4$ surface.[15,42,43] The adsorbed polymer layer, which can act as a good electronic conductor, inhibits the surface reaction of Mn dissolution and thus reduces the degradation of spinel electrode. As a result, the chemically modified $LiMn_2O_4$ with organic polymer displays an improved cycling stability at room and high temperatures and it extends the lifetime of the active material.

The causes for the enhanced electrochemical performance of the chemically/surface modified $LiMn_2O_4$ can be summarised as follows : (i) the surface film formed on $LiMn_2O_4$ surface prevents the direct contact between the spinel and electrolyte, which suppresses $Mn^{3+}$ dissolution responsible for the capacity fading,[8-10,12,13] (ii) coated materials reduce the concentration of HF in the electrolyte by neutralisation,[41] (iii) modifying ions diffuse into $LiMn_2O_4$ lattice during heat treatment and then suppress the phase transition by occupying the vacant cationic sites and finally prevent a vacancy disorder at high potentials,[11] and (iv) coated polymers enhance the electronic and ionic conductivities of $LiMn_2O_4$.[15,42,43] From the practical use as a cathode material of lithium ion batteries, the chemically/surface modified spinel $LiMn_2O_4$ will be attractive due to its high rate capability and excellent cycling behaviour at room and high temperatures.

## 4. Kinetics of Lithium Transport through Chemically/Surface Modified $Li_{1-\delta}Mn_2O_4$ Electrode

Until now we presented the comprehensive survey of the cubic spinel structure and its correlated electrochemical behaviour of $LiMn_2O_4$. Then, we summarised the various kinds of the chemically modified $LiMn_2O_4$ electrode and their electrochemical performance reported by many researchers. Now we reviewed the kinetics of lithium transport through the chemically modified $Li_{1-\delta}Mn_2O_4$ electrode and transition of transport mechanism by analyses of the current transient and ac-impedance spectra based upon our recent works.[44,45]

Fig. 5 shows the electrode potentials obtained from the galvanostatic intermittent discharge curves of the unmodified and chemically modified $Li_{1-\delta}Mn_2O_4$ with $LiCoO_2$ film electrodes prepared by using rf-sputtering system in a 1 M $LiClO_4$–PC solution as a function of the lithium content. The electrode potential curves exhibit two potential plateaux near 4.0 and 4.125 $V_{Li/Li+}$. Especially, the appearance of two potential plateaux in the electrode potential curves strongly indicates that the order to disorder phase transitions occur due

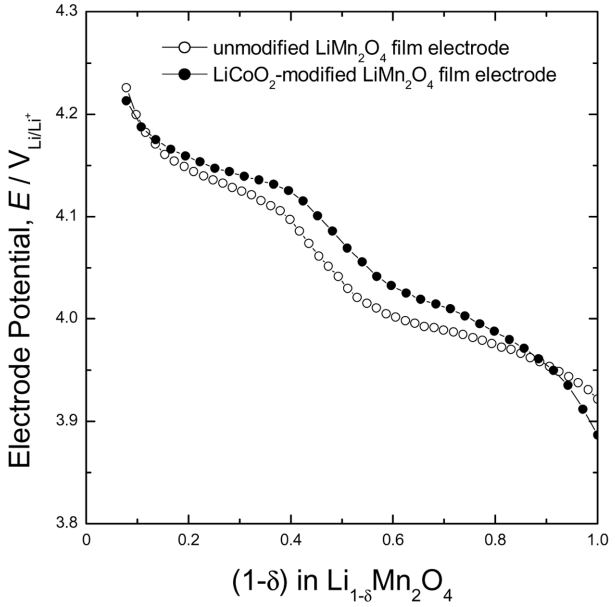


**Fig. 5. Electrode potentials obtained from the galvanostatic intermittent discharge curves as a function of the lithium content (1-δ) measured on the unmodified and chemically modified $Li_{1-\delta}Mn_2O_4$ with $LiCoO_2$ film electrodes.**

to the interactions between lithium ions in the $Li_{1-\delta}Mn_2O_4$ electrode.[20-22,46,47] From the result of the electrode potential curves, it is quite reasonable to say that the $LiCoO_2$-modified $Li_{1-\delta}Mn_2O_4$ film electrode shows the same character as the unmodified $Li_{1-\delta}Mn_2O_4$ film electrode.

Fig. 6(a) and (b) gives on a logarithmic scale the cathodic current transients obtained from the unmodified and $LiCoO_2$-modified $Li_{1-\delta}Mn_2O_4$ film electrodes in a 1 M $LiClO_4$-PC solution by dropping the electrode potential of 4.25 $V_{Li/Li+}$ to various lithium injection potentials, respectively. All the current transients measured from both the electrodes scarcely show the Cottrell behaviour,[48] viz. there is no clear linear relationship between the logarithm of current and the logarithm of time with a slope of -0.5 in the early stage. In Fig. 6(c), it was also found that the initial current $I_{ini}$ obtained at 0.22 s from the measured current transient of both the electrodes is linearly proportional to the potential drop $\Delta E$, indicating that the relationship between $I_{ini}$ and $\Delta E$ just holds Ohm's law.

In our previous works[46,47,49-52] on the current transients obtained from transition metal oxides, it was suggested that the occurrence of both the non-Cottrell behaviour of the current transient and ohmic relationship between $I_{ini}$ and $\Delta E$ is responsible for the cell-impedance-controlled lithium transport. Therefore, it seems to be reasonable to say that lithium transport through the chemically modified $Li_{1-\delta}Mn_2O_4$ electrode as well as lithium transport through the unmodified $Li_{1-\delta}Mn_2O_4$ electrode proceeds by the same mechanism involving the cell-impedance-controlled constraint as follows[51]:

$$I_{int}(t) = -zF\tilde{D}_{Li}A_{ea}\left(\frac{\partial c}{\partial x}\right)_{x=0} = \frac{E_{app} - E(t)}{R_{int}} \quad (2)$$

where $I_{int}$ is the cell-impedance-controlled current, $z$ the

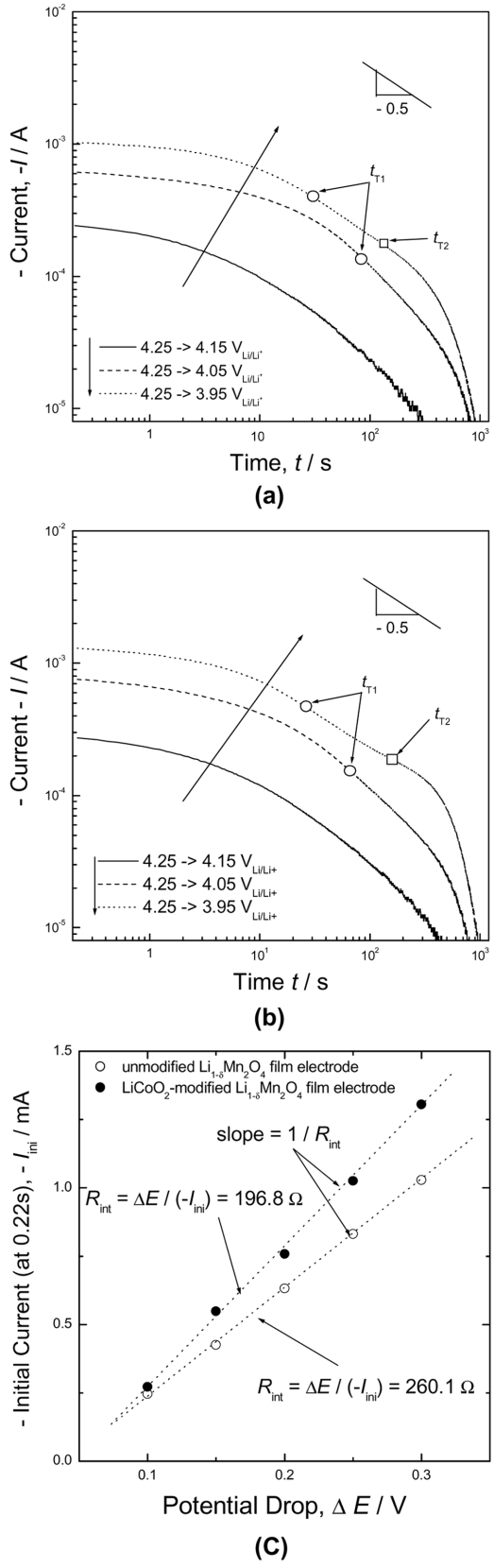


**Fig. 6. Cathodic current transients on a logarithmic scale obtained from (a) the unmodified and (b) chemically modified $Li_{1-\delta}Mn_2O_4$ with $LiCoO_2$ film electrodes in a 1 M $LiClO_4$-PC solution at the potential drops from the initial electrode potential 4.25 $V_{Li/Li+}$ to various lithium injection potentials, and (c) plots of the initial current $I_{ini}$ at 0.22 s against the potential drop $\Delta E$.**

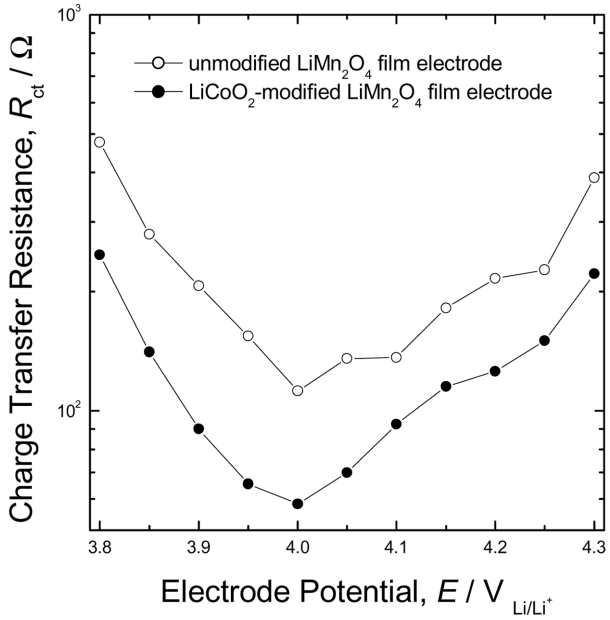


**Fig. 7. Plots of the charge-transfer resistance $R_{ct}$ against the electrode potential, obtained from the unmodified and chemically modified $Li_{1-\delta}Mn_2O_4$ with $LiCoO_2$ film electrodes in a 1 M $LiClO_4$-PC solution at 25°C by using electrochemical impedance spectroscopy (EIS).**

valence number, $F$ the Faraday constant, $\tilde{D}_{Li}$ the chemical diffusivity of lithium, $A_{ea}$ the electrochemical active area, $c$ the local concentration of lithium, $x$ the distance into the electrode from the electrode/electrolyte interface, $E_{app}$ the applied potential (lithium extraction potential), $E(t)$ the electrode potential and $R_{int}$ represents the internal cell resistance.

In order to clearly elucidate the effect of the surface-modification on lithium transport through the chemically modified $Li_{1-\delta}Mn_2O_4$ electrode, the value of the charge-transfer resistance $R_{ct}$ was determined by analysis of the ac-impedance spectra obtained from the unmodified and $LiCoO_2$-modified $Li_{1-\delta}Mn_2O_4$ film electrodes, and the resulting values are plotted as a function of the electrode potential $E$ in Fig. 7. It was found that the $R_{ct}$ values of both the electrodes are strongly dependent upon $E$. In addition, it should be noted that $R_{ct}$ determined from the chemically modified $Li_{1-\delta}Mn_2O_4$ electrode is lower in value than $R_{ct}$ determined from the unmodified $Li_{1-\delta}Mn_2O_4$ electrode over the whole potential range.

It is known[53] that the charge-transfer reaction may significantly depend upon the surface properties of the electrode and may also be strongly affected by the surface film covering the electrode surface. Consequently, it is recognised that the considerable decrease of $R_{ct}$ obtained from the $LiCoO_2$-modified $Li_{1-\delta}Mn_2O_4$ can be attributable to the kinetic facilitation of the interfacial charge-transfer reaction in the presence of the more conductive $LiCoO_2$ surface film.

Fig. 8(a) illustrates the typical Nyquist plot of the ac-impedance spectra measured on the unmodified and chemically modified $Li_{1-\delta}Mn_2O_4$ with metal oxides such as $Al_2O_3$, MgO and $ZnO_2$ composite electrodes at 4.0 $V_{Li/Li+}$ in a 1 M $LiPF_6$-EC/DEC solution. It was found that the magnitudes of the first and the second arcs of the ac-impedance spectra

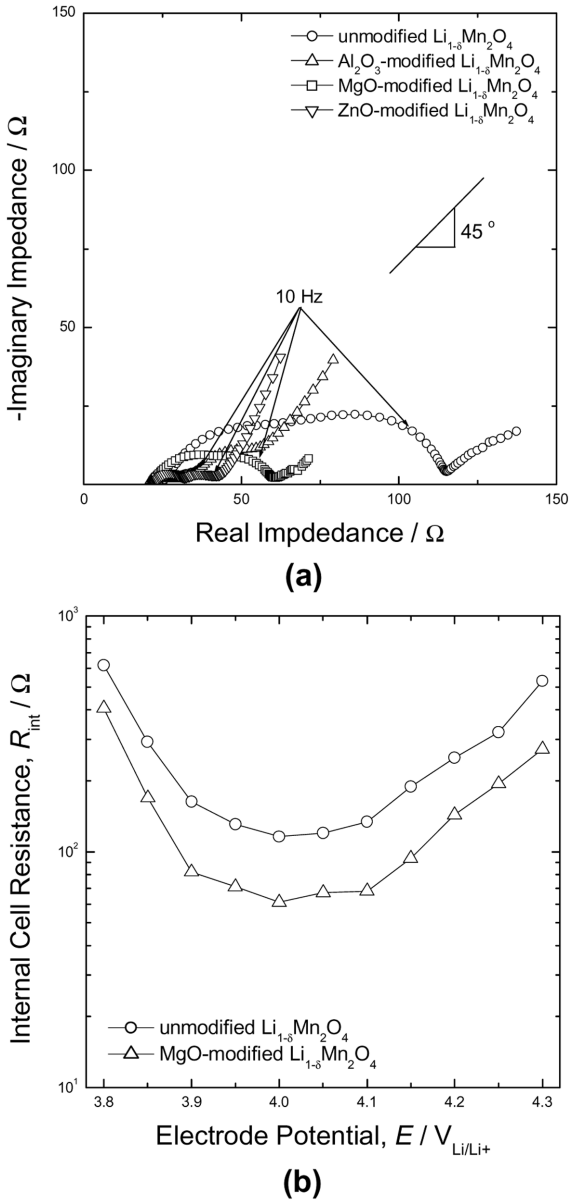


**Fig. 8. (a) Nyquist plots of the ac-impedance spectra obtained from the unmodified and chemically-modified $Li_{1-\delta}Mn_2O_4$ with metal oxides such as $Al_2O_3$, MgO and ZnO composite electrodes at 4.0 $V_{Li/Li+}$ and (b) plots of the internal cell resistance $R_{int}$ against the electrode potential obtained from the unmodified and chemically modified $Li_{1-\delta}Mn_2O_4$ composite electrodes with MgO in a 1 M $LiPF_6$-EC/DEC solution at 25°C.**

obtained from the chemically modified electrodes are much smaller than those of the unmodified electrode. This result is similar to that ac-impedance spectra obtained from the $LiCoO_2$-modified $Li_{1-\delta}Mn_2O_4$ film electrode.[44]

It is generally accepted[53] that the first arc is mainly caused by the formation of the passive film on the electrode surface and the second arc is ascribed to the charge-transfer reaction at the interface between the surface film and electrode. The values of the internal cell resistance determined from the unmodified and MgO-modified $Li_{1-\delta}Mn_2O_4$ composite electrodes are plotted against the electrode potential in Fig. 8(b). Here, the internal cell resistance means the sum of the

uncompensated ohmic resistance of the electrolyte, surface film resistance and charge-transfer resistance at the electrolyte/electrode interface. From those results, the beneficial contribution of the surface-modification to lithium transport through the chemically modified $Li_{1-\delta}Mn_2O_4$ electrode was again confirmed.

In our previous works on lithium transport through transition metal oxide electrodes,[44,54,55] it was suggested that for the large potential jump and the small change of lithium amount transferred during lithium transport, the cell-impedance-controlled constraint at the electrode surface changes to the diffusion-controlled constraint. In order to compare the transition of transport mechanism in the unmodified and chemically modified $Li_{1-\delta}Mn_2O_4$ electrodes, the anodic current transients were experimentally determined. Fig. 9(a) and (b) illustrates on a logarithmic scale the anodic current transients experimentally obtained from the unmodified and $LiCoO_2$-modified $Li_{1-\delta}Mn_2O_4$ film electrodes, respectively, in a 1 M $LiClO_4$-PC solution by jumping the initial potential, $E_{ini}$, 4.15 $V_{Li/Li+}$ to various lithium extraction potentials, $E_{ext}$, in the range of 4.25 to 5.20 $V_{Li/Li+}$.

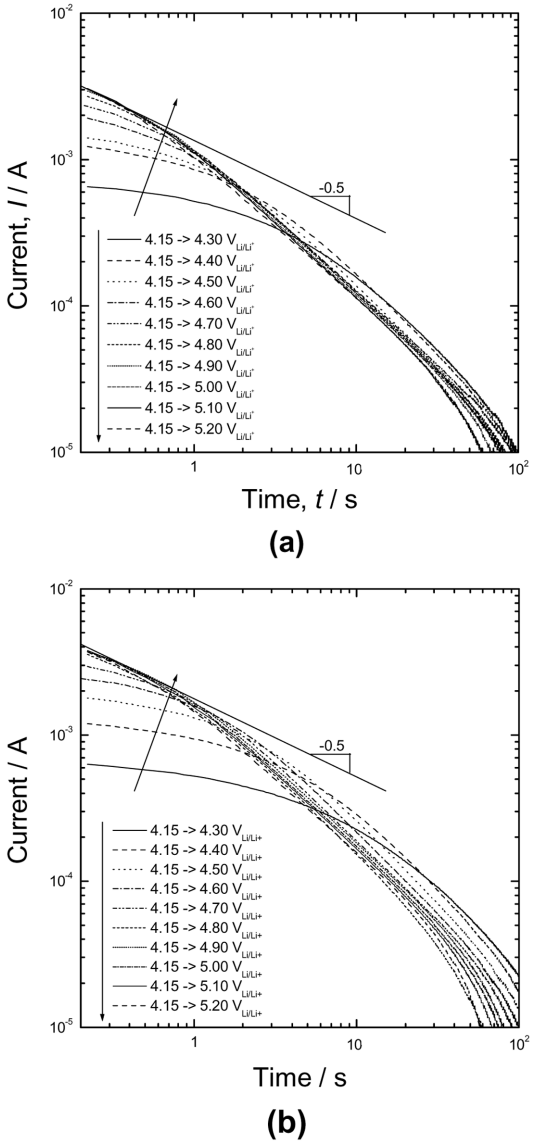


**Fig. 9. Anodic current transients experimentally obtained from (a) the unmodified and (b) chemically modified $Li_{1-\delta}Mn_2O_4$ with $LiCoO_2$ film electrodes in a 1 M $LiClO_4$-PC solution at the potential jumps from the initial electrode potential 4.15 $V_{Li/Li+}$ to various lithium extraction potentials.**

Fig. 9(a) and (b) indicates that the anodic current transients obtained from the unmodified and $LiCoO_2$-modified $Li_{1-\delta}Mn_2O_4$ film electrodes follow the Ohmic behaviour in the value of $E_{ext}$ lower than 4.8 $V_{Li/Li+}$, viz., the initial current level $I_{ini}$ is proportional to the potential step and the instantaneous current value decreases monotonically with time on a logarithmic scale. In contrast, the current transients follow the Cottrell behaviour in the value of $E_{ext}$ higher than 4.8 $V_{Li/Li+}$, viz., a linear relationship between the logarithm of current and the logarithm of time with a slope of -0.5, and after a certain time, the logarithm of current simply decays with the logarithm of time. Moreover, the current transients share in shape and value with one another, since the amount of lithium transferred during the potential jump has an almost constant value irrespective of the value of $E_{ext}$.

The values of $I_{ini}$ taken at 0.22 s from the anodic current transients of Fig. 9(a) and (b) are plotted against the lithium extraction potential $E_{ext}$ in Fig. 10(a) and (b), respectively. The value of $I_{ini}$ experimentally determined from the unmodified and $LiCoO_2$-modified $Li_{1-\delta}Mn_2O_4$ film electrodes increases linearly with rising $E_{ext}$ up to 4.80 $V_{Li/Li+}$ and 4.75 $V_{Li/Li+}$, respectively, and then remains nearly constant. In order to more clearly specify which boundary condition is established at the electrode surface, the values of $I_{ini}$ obtained experimentally from the anodic current transients are compared with those values calculated theoretically under the diffusion-controlled constraint as well as under the cell-impedance-controlled constraint. The diffusion-controlled current $I_D$ was determined in value from the Cottrell equation[48] and the cell-impedance-controlled current $I_{int}$ was calculated in value from the Ohm's law given as Eq. (2). The resulting values of $I_{int}$ and $I_D$ are designated in Fig. 10(a) and (b) as open triangles(△) and open squares(□), respectively.

The transition potential $E_{tr}$ is defined as the extraction potential at which the plot of $I_{int}$ versus $E_{ext}$ calculated from the Ohm's law intersects the plot of $I_D$ versus $E_{ext}$ calculated from the Cottrell equation, and it was determined in value to be ca. 4.87 $V_{Li/Li+}$ and 4.82 $V_{Li/Li+}$, respectively, from Fig. 10(a) and (b). It is seen that the measured $I_{ini}$ is almost identical to $I_{int}$ calculated from the Ohm's law in the value of $E_{ext}$ lower than $E_{tr}$, which means that the cell-impedance-controlled constraint is effective at the electrode surface for lithium transport. On the other hand, the measured $I_{ini}$ coincides fairly well with $I_D$ calculated from the Cottrell equation in the value of $E_{ext}$ higher than $E_{tr}$, implying that the diffusion-controlled constraint is satisfied at the electrode surface.

The results of the current transients determined from the MgO-modified $Li_{1-\delta}Mn_2O_4$ composite electrode[45] are similar to those current transients obtained from the $LiCoO_2$-modified $Li_{1-\delta}Mn_2O_4$ film electrode. Fig. 11(a) and (b) presents the anodic current transients on a logarithmic scale experimentally obtained from the unmodified and MgO-modified $Li_{1-\delta}Mn_2O_4$

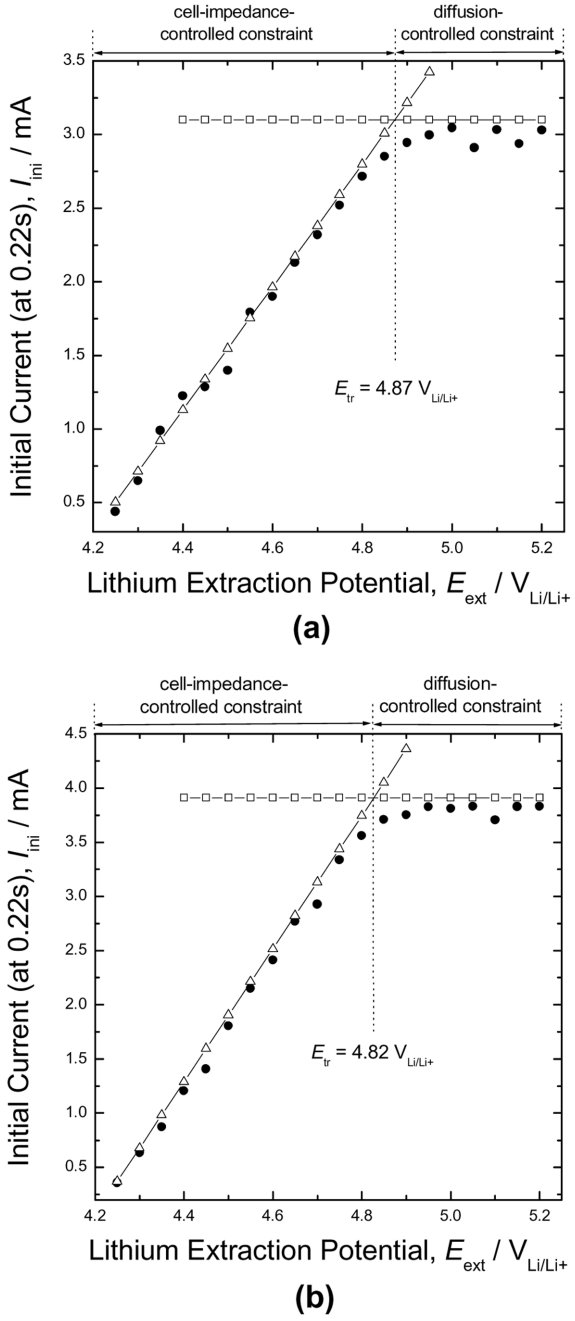


**Fig. 10. Plots of the initial current level against the lithium extraction potential (●) experimentally measured from the current transient of (a) the unmodified and (b) chemically modified $Li_{1-\delta}Mn_2O_4$ with $LiCoO_2$ film electrodes in a 1 M $LiClO_4$-PC solution; (△) calculated from Ohm's law; (□) calculated by the Cottrell equation.**

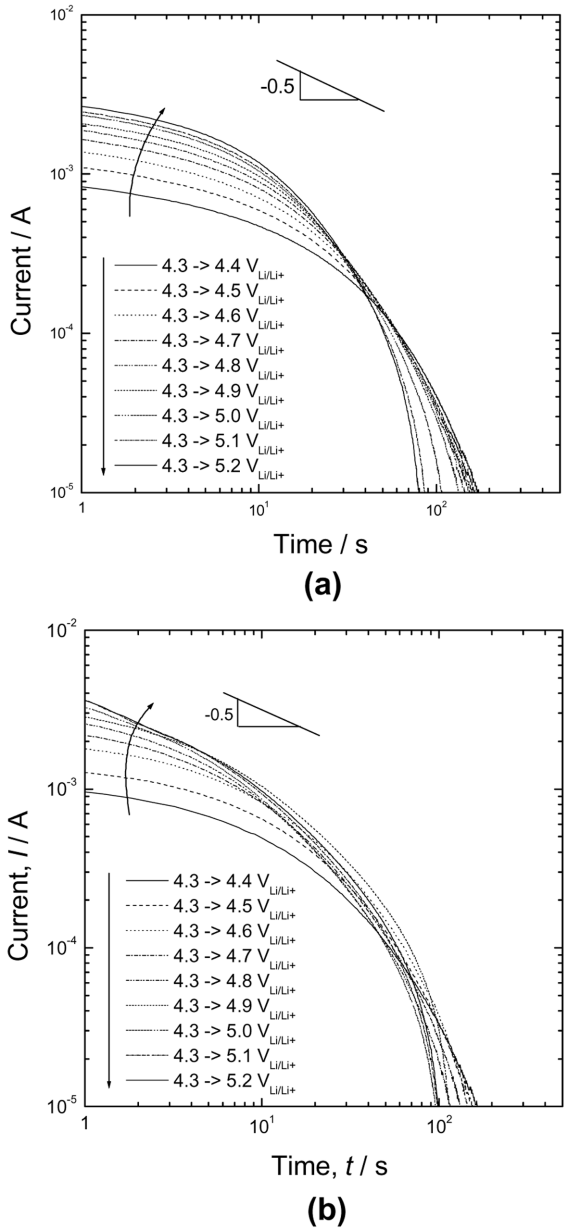


**Fig. 11. Anodic current transients on a logarithmic scale experimentally obtained from (a) the unmodified and (b) chemically-modified $Li_{1-\delta}Mn_2O_4$ with MgO composite electrodes in a 1 M $LiPF_6$-EC/DEC solution at the potential jumps from the initial electrode potential $E_{ini}$ of 4.3 $V_{Li/Li+}$ to various lithium extraction potentials $E_{ext}$.**

composite electrodes, respectively, in a 1 M $LiPF_6$-EC/DEC solution by jumping the initial potential $E_{ini}$ of 4.3 $V_{Li/Li+}$ to various lithium extraction potentials $E_{ext}$ in the range of 4.4 to 5.2 $V_{Li/Li+}$. All the anodic current transients obtained from the unmodified $Li_{1-\delta}Mn_2O_4$ composite electrode follow the Ohmic behaviour, and the instantaneous current value decreases monotonically with time on a logarithmic scale as shown in Fig. 11(a).

Fig. 11(b) indicates that the anodic current transients obtained from the MgO-modified $Li_{1-\delta}Mn_2O_4$ electrode follow the Ohmic behaviour in the range of $E_{ext}$ lower than 4.9 $V_{Li/Li+}$. As against, they follow the Cottrell behaviour in the range of $E_{ext}$ higher than 4.9 $V_{Li/Li+}$, and after a certain time, the logarithm of current decays exponentially with the logarithm of time. Moreover, the current transients share in shape and value with each other, since the amount of lithium transferred during the potential jump has almost a constant value irrespective of the $E_{ext}$ value.

The values of initial current taken at 1.07 s from the anodic current transients of Fig. 11(a) and (b) are plotted against the lithium extraction potential $E_{ext}$ in Fig. 12(a) and (b), respec-

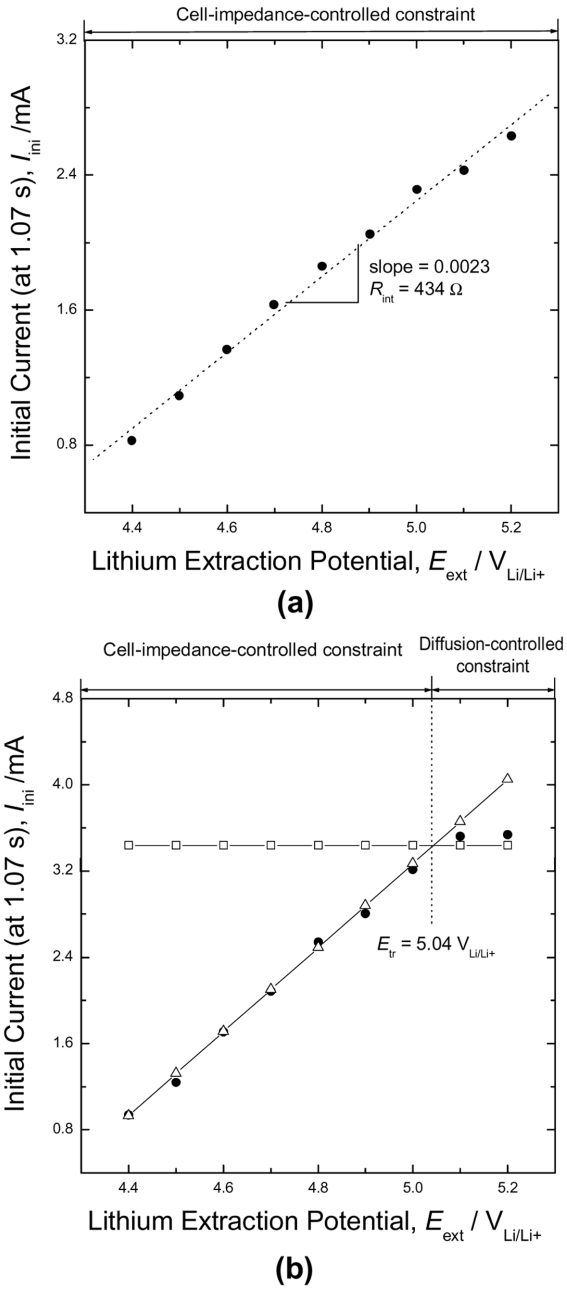


**Fig. 12. Plots of the initial current level against the lithium extraction potential experimentally determined (●) from the current transients of (a) the unmodified and (b) chemically-modified $Li_{1-\delta}Mn_2O_4$ with MgO composite electrodes in a 1 M $LiPF_6$-EC/DEC solution; (△) calculated from Ohm's law; (□) calculated by the Cottrell equation.**

tively. In Fig. 12(a), it was found that the initial current $I_{ini}$ experimentally determined from the unmodified $Li_{1-\delta}Mn_2O_4$ composite electrode is linearly proportional to the potential jump $\Delta E$. Therefore, it seems to be reasonable to say that lithium transport through the unmodified $Li_{1-\delta}Mn_2O_4$ composite electrode proceeds by the cell-impedance-controlled constraint.

On the other hand, in Fig. 12(b), the value of $I_{ini}$ experimentally determined from the MgO-modified $Li_{1-\delta}Mn_2O_4$ composite electrode increases linearly with rising $E_{ext}$ up to 4.9 $V_{Li/Li+}$ and then remains nearly constant. The values of $I_{ini}$ obtained experimentally from the anodic current transients are compared with those values calculated theoretically under the diffusion-controlled as well as under the cell-impedance-controlled constraint. $I_D$ was determined in value from the well-known Cottrell equation in the case of spherical electrode[56] and $I_{int}$ was calculated in value from the Ohm's law given as Eq. (2).

The resulting values of $I_{int}$ and $I_D$ are designated in Fig. 12(b) as open triangles(△) and open squares(□), respectively. The transition potential $E_{tr}$ was determined in value to be ca 5.04 $V_{Li/Li+}$. It was found that the measured $I_{ini}$ is almost identical to $I_{int}$ calculated from Eq. (2) in the range of $E_{ext}$ lower than $E_{tr}$, which means that the cell-impedance-controlled constraint is effective at the electrode surface for lithium transport. By contrast, the measured $I_{ini}$ coincides fairly well with $I_D$ calculated from the Cottrell equation in the range of $E_{ext}$ higher than $E_{tr}$, implying that the diffusion-controlled constraint is satisfied at the electrode surface.

In addition, it was reported[45] that the internal cell resistance of the MgO-modified $Li_{1-\delta}Mn_2O_4$ composite electrode determined at 298 K reduced with reference to the unmodified $Li_{1-\delta}Mn_2O_4$ composite electrode at 298 K shows almost a similar value to that of the unmodified $Li_{1-\delta}Mn_2O_4$ composite electrode determined at 313 K. Nevertheless, it was found that the mechanism transition of lithium transport occurs through the MgO-modified $Li_{1-\delta}Mn_2O_4$ electrode at 298 K, but it does not occur through the unmodified $Li_{1-\delta}Mn_2O_4$ electrode at 313 K. According to the cell-impedance-controlled model, lithium transport through transition metal oxide proceeds under the condition in which the cell-impedance-controlled reaction at the electrolyte/electrode interface is coupled with diffusion of lithium in the bulk electrode. Thus, one of the most plausible reasons for the invariance of the transport mechanism at 313 K may be from the fact that the diffusion resistance $R_D$ in the electrode as well as the internal cell resistance $R_{int}$ is strongly affected by temperature.

In this respect, the temperature dependence of the diffusion resistance $R_D$ in the bulk electrode were calculated from the chemical diffusivity of lithium $\tilde{D}_{Li}$ according to the well-known equation[47,48,52]:

$$R_D = \frac{R^* V_m}{F \tilde{D}_{Li} A_{ea}} \left( \frac{dE}{d(1-\delta)} \right) \quad (3)$$

where $R^*$ is the average radius of $LiMn_2O_4$ particle, $V_m$ the molar volume of the electrode and $dE/d(1-\delta)$ represents the slope of $E$ versus $(1-\delta)$ curve. Here, the chemical diffusivities of lithium $\tilde{D}_{Li}$ in the bulk electrode at various temperatures were estimated from the potential transient and coulometric titration curve by galvanostatic current transient technique.

Fig. 13 envisages the values of $R_D$ on a logarithmic scale against the electrode potential determined from the unmodified $Li_{1-\delta}Mn_2O_4$ composite electrode at various temperatures. All the plots of $R_D$ against the electrode potential coincide satisfactorily in shape with one another, showing two minima at approximately 3.98 and 4.13 $V_{Li/Li+}$. Particularly, it should be noted that the values of $R_D$ decrease as a whole with

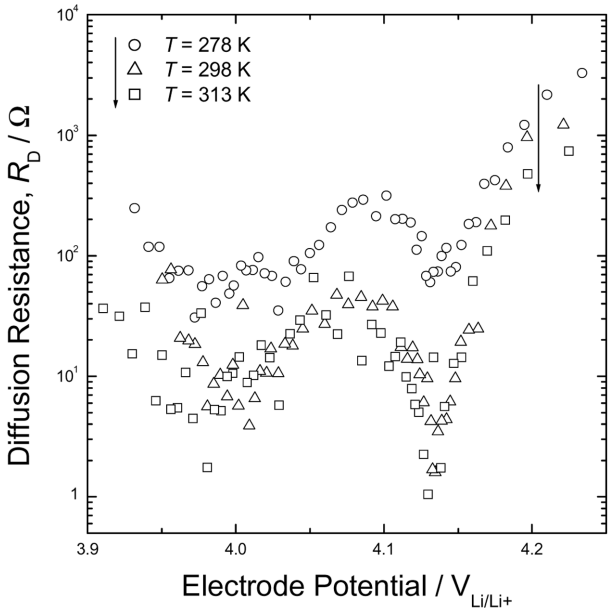


**Fig. 13. Plots of the diffusion resistance of lithium $R_D$ on a logarithmic scale with respect to the electrode potential obtained from the unmodified $Li_{1-\delta}Mn_2O_4$ composite electrode in a 1 M $LiPF_6$-EC/DEC solution at various temperatures by using galvanostatic intermittent titration technique (GITT).**

increasing temperature, implying that the chemical diffusivity of lithium $\tilde{D}_{Li}$ in the bulk electrode increases with increasing temperature.

In the previous works,[44,51,54,55] it was suggested that $R_D$ of the unmodified electrode should necessarily be much larger in value than $R_{int}$ and simultaneously $I_D$ should be lower in value than $I_{int}$, if the mechanism transition at 313 K occurred from the cell-impedance-controlled to diffusion-controlled constraint which means the diffusion-controlled boundary condition were effective at the electrode surface. In reality, however, it does not occur. This can be accounted for in the following way. $R_{int}$ and $R_D$ decrease as well in value with increasing temperature.[45] From this, it is conceivable that the contribution of reduction in $R_{int}$ to the mechanism transition at the unmodified $Li_{1-\delta}Mn_2O_4$ electrode at 313 K is comparable with that contribution of reduction in $R_D$.

From the analyses of the anodic current transients and ac-impedance spectra obtained from the unmodified and surface-modified $Li_{1-\delta}Mn_2O_4$ electrodes, it was found that the cell-impedance-controlled constraint at the electrode surface is changed to the diffusion-controlled constraint. Considering that the internal cell resistance of the surface-modified electrode is considerably reduced in value compared to that of the unmodified electrode, it is reasonable to say that the mechanism transition of lithium transport through the chemically/surface modified $Li_{1-\delta}Mn_2O_4$ electrode readily occurs. This is due mainly to the fact that the applied potential step needed for the mechanism transition is considerably reduced by the surface-modification of the electrode surface.

In addition, from the temperature dependences of the internal cell resistance and diffusion resistance measured on the unmodified $Li_{1-\delta}Mn_2O_4$ composite electrode, it was experimentally recognised that the diffusion resistance as well as the internal cell resistance plays an important role in the determination of the boundary condition at the electrode surface. This means which one dominates the other of the transport mechanism and vice versa is not fixed at the specific electrode system by itself, but it depends even at any electrode system upon the combined applied potential step and the external parameters such as the internal cell resistance and diffusion resistance during lithium transport.[54]

## 5. Concluding Remarks

The present article first explained the cubic spinel structure and its correlated electrochemical behaviour of $LiMn_2O_4$. Then, this article described the various kinds of the chemically/surface modified $LiMn_2O_4$ in relation to the electrochemical behaviour. Finally, this article reviewed our recent research works on the mechanism of lithium transport through chemically/surface modified $Li_{1-\delta}Mn_2O_4$ electrode from the kinetic view point by the analyses of the potentiostatic current transients and ac-impedance spectra.

In our recent work, it was found that lithium transport through the chemically modified $Li_{1-\delta}Mn_2O_4$ electrode is governed by the cell-impedance-controlled constraint, and at the same time lithium transport through the chemically modified electrode is markedly enhanced due to the kinetic facilitation of the interfacial reaction. Moreover, it was also recognised that the internal cell resistance as well as the diffusion resistance plays a key role in the determination of the boundary condition at the electrode surface.

## Acknowledgements

The receipt of a research grant from the Center for Advanced Materials Processing (CAMP) of the 21st Century Frontier R&D Programme, funded by Ministry of Commerce, Industry and Energy, Republic of Korea, is gratefully acknowledged.

## References

1. J. M. Tarascon and D. Guyomard, *Electrochim. Acta*, **38**, 1221 (1993).
2. M. M. Thackeray, *Prog. Solid State Chem.*, **25**, 1 (1997).
3. V. Manev, B. Banov, A. Momchiler, and A. Nassalevska, *J. Power Sources*, **57**, 99 (1995).
4. P. Arora, R. E. White, and M. Doyle, *J. Electrochem. Soc.*, **145**, 3647 (1998).
5. R. J. Gummow, A de Kock, and M. M. Thackeray, *Solid State Ionics*, **69**, 59 (1994).
6. F. Le Cras, D. Bloch, M. Anne, and P. Strobel, *Solid State Ionics*, **89**, 203 (1996).
7. L. Guohua, H. Ikuta, T. Uchida, and M. Wakihara, *J. Electrochem. Soc.*, **143**, 178 (1996).
8. G. G. Amatucci, A. Blyr, C. Sigala, P. Alfonse, and J. M. Tarascon, *Solid State Ionics*, **104**, 13 (1997).
9. Q. Zhong, A. Bonakdarpour, M. Zhang, Y. Gao, and J.R. Dahn, *J. Electrochem. Soc.*, **144**, 205 (1997).
10. J. Cho, G. B. Kim, H. S. Lim, C. S. Kim, and S. I. Yoo,

*Electrochem. Solid-State Lett.*, **2**, 607 (1999).
11. A. M. Kannan and A. Manthiram, *Electrochem. Solid-State Lett.*, **5**, A167 (2002).
12. Z. Liu, H. Wang, L. Fang, J. Y. Lee, and L. M. Gan, *J. Power Sources*, **104**, 101 (2002).
13. J. S. Gnanaraj, V. G. Pol, A. Gedanken, and D. Aurbach, *Electrochem. Commun.*, **5**, 940 (2003).
14. D. Shu, G. Kumar, K. B. Kim, K. S. Ryu, and S. H. Chang, *Solid State Ionics*, **160**, 227 (2003).
15. R. Vidu and P. Stroeve, *Ind. Eng. Chem. Res.*, **43**, 3314 (2004).
16. L. J. Fu, H. Liu, C. Li, Y. P. Wu, E. Rahm, R. Holze, and H. Q. Wu, *Solid State Sci.*, **8**, 113 (2006).
17. C. Li, H. P. Zhang, L. J. Fu, H. Liu, Y. P. Wu, E. Rahm, R. Holze, and H. Q. Wu, *Electrochim. Acta*, **51**, 3872 (2006).
18. M. M. Thackeray, M. H. Rossouw, A. de Kock, A. P. de la Harpe, R. K. Gummow, K. Pearce, and D. C. Liles, *J. Power Sources*, **43-44**, 289 (1993).
19. T. Ohzuku, M. Kitagawa, and T. Hirai, *J. Electrochem. Soc.*, **137**, 169 (1990).
20. Y. Gao, J. N. Reimers, and J. R. Dahn, *Phys. Rev. B*, **54**, 3878 (1996).
21. H. Abiko, M. Hibino, and T. Kudo, *Electrochem. Solid-State Lett.*, **1**, 114 (1998).
22. T. Kudo and M. Hibino, *Electrochim. Acta*, **43**, 781 (1998).
23. W. I. F. David, M. M. Thackeray, L. A. de Picciotto, and J. B. Goodenough, *J. Solid State Chem.*, **67**, 316 (1987).
24. M. M. Thackeray, P. J. Johnson, L. A. de Picciotto, P. G. Bruce, and J. B. Goodenough, *Mat. Res. Bull.*, **19**, 179 (1984).
25. G. G. Amatucci, N. Pereira, T. Zheng, and J. M. Tarascon, *J. Electrochem. Soc.*, **148**, A171 (2001).
26. P. R. Moses, L. Wier, and R. W. Murray, *Anal. Chem.*, **47**, 1882 (1975).
27. R. W. Murray, *Acc. Chem. Res.*, **13**, 135 (1980).
28. R. W. Murray, A. G. Ewing, and R. A. Durst, *Anal. Chem.*, **59**, 379A (1987).
29. A. M. Titse, A. M. Timinov, and G. A. Shagisultanova, *Coord. Chem. Rev.*, **125**, 43 (1993).
30. S. Flink, F. C. J. M. van Veggel, and D. N. Reinhoudt, *Adv. Mat.*, **12**, 1315 (2000).
31. L. Kavan, *Chem. Rev.*, **97**, 3061 (1997).
32. A. J. Downard, *Electroanalysis*, **12**, 1085 (2000).
33. J. Zak and T. Kuwana, *J. Am. Chem. Soc.*, **104**, 5514 (1982).
34. C. J. Miller and M. Majda, *J. Am. Chem. Soc.*, **107**, 1419 (1985).
35. P. K. Ghosh and A. J. Bard, *J. Am. Chem. Soc.*, **105**, 5591 (1983).
36. A. Walcarius, *Electroanalysis*, **8**, 971 (1996).
37. V. Stara and M. Kopanica, *Electroanalysis*, **1**, 251 (1989).
38. K. Kalcher, *Electroanalysis*, **2**, 419 (1990).
39. J. Wang, *Electroanalysis*, **3**, 255 (1991).
40. D. Guyomard and J. M. Tarascon, *J. Power Sources*, **54**, 92 (1995).
41. M. M. Thackeray, C. S. Johnson, J. S. Kim, K. C. Lauzze, J. T. Vaughey, N. Dietz, D. Abraham, S. A. Hackney, W. Zeltner, and M. A. Anderson, *Electrochem. Commun.*, **5**, 752 (2003).
42. M. Nishizawa, K. Mukai, S. Kuwabata, C. R. Martin, and H. T. Yoneyama, *J. Electrochem. Soc.*, **144**, 1923 (1997).
43. C. Arbizznani, M. Mastragostino, and M. Rossi, *Electrochem. Commun.*, **4**, 545 (2002).
44. K.-H. Kim, S.-I. Pyun, and K.-N. Jung, *Electrochim. Acta*, **52**, 152 (2006).
45. K.-N. Jung and S.-I. Pyun, submitted to *Electrochim. Acta* (2006).
46. S.-W. Kim and S.-I. Pyun, *Electrochim. Acta*, **47**, 2843 (2002).
47. S.-W. Kim and S.-I. Pyun, *J. Electroanal. Chem.*, **528**, 114 (2002).
48. C. J. Wen, B. A. Boukamp, R.A. Huggins, and W. Weppner, *J. Electrochem. Soc.*, **126**, 2258 (1979).
49. J.-Y. Go, S.-I. Pyun, and H.-C. Shin, *J. Electroanal. Chem.*, **527**, 93 (2002).
50. J.-W. Lee and S.-I. Pyun, *J. Power Sources*, **119-121**, 760 (2003).
51. H.-C. Shin and S.-I. Pyun, "Mechanisms of Lithium Transport through Transition Metal Oxides and Carbonaceous Materials". In: C. G. Vayenas, B. E. Conway, R.E. White (eds), Modern Aspects of Electrochemistry, **No. 36, Ch. 5**, Kluwer Academic Publishers/ Plenum Press, New York (2003), pp. 255-301.
52. J.-W. Lee and S.-I. Pyun, *Electrochim. Acta*, **49**, 753 (2004).
53. D. Aurbach, K. Gamolsky, B. Markovsky, G. Salitra, Y. Gofer, U. Heider, R. Oesten, and M. Schmidt, *J. Electrochem. Soc.*, **147**, 1322 (2000).
54. J.-Y. Go and S.-I. Pyun, *Electrochim. Acta*, **49**, 2551 (2004).
55. K.-N. Jung and S.-I. Pyun, *Electrochim. Acta*, **49**, 4371 (2004).
56. D. D. Macdonald, "Transient Techniques in Electrochemistry", Plenum Press, New York (1977), pp. 73.